Cardiovasc Intervent Radiol (2011) 34:989–997
DOI 10.1007/s00270-010-0048-z

CLINICAL INVESTIGATION

Lung Tumors Treated With Percutaneous Radiofrequency Ablation: Computed Tomography Imaging Follow-Up

Jean Palussière · Benjamin Marcet · Edouard Descat · Frédéric Deschamps · Pramod Rao · Alain Ravaud · Véronique Brouste · Thierry de Baère

Received: 2 July 2010 / Accepted: 24 October 2010 / Published online: 3 December 2010

Abstract
Purpose To describe the morphologic evolution of lung tumors treated with radiofrequency ablation (RFA) by way of computed tomography (CT) images and to investigate patterns of incomplete RFA at the site of ablation.
Materials and Methods One hundred eighty-nine patients with 350 lung tumors treated with RFA underwent CT imaging at 2, 4, 6, and 12 months. CT findings were interpreted separately by two reviewers with consensus. Five different radiologic patterns were predefined: fibrosis, cavitation, nodule, atelectasis, and disappearance. The appearance of the treated area was evaluated at each follow-up CT using the predefined patterns.
Results At 1 year after treatment, the most common evolutions were fibrosis (50.5%) or nodules (44.8%). Differences were noted depending on the initial size of the tumor, with fibrosis occurring more frequently for tumors <2 cm (58.6% vs. 22.9%, $P = 1 \times 10^{-5}$). Cavitation and atelectasis were less frequent patterns (2.4% and 1.4%, respectively, at 1 year). Tumor location (intraparenchymatous, with pleural contact <50% or >50%) was not significantly correlated with follow-up image pattern. Local tumor progressions were observed with each type of evolution. At 1 year, 12 local recurrences were noted: 2 cavitations, which represented 40% of the cavitations noted at 1 year; 2 fibroses (1.9%); 7 nodules (7.4%); and 1 atelectasis (33.3%).
Conclusion After RFA of lung tumors, follow-up CT scans show that the shape of the treatment zone can evolve in five different patterns. None of these patterns, however, can confirm the absence of further local tumor progression at subsequent follow-up.

J. Palussière (✉) · B. Marcet · E. Descat
Department of Interventional Radiology,
Institut Bergonié, Regional Cancer Center,
229 cours de l'Argonne, 33076 Bordeaux Cedex, France
e-mail: palussiere@bergonie.org

A. Ravaud
Department of Medical Oncology, Hôpital Saint-André,
1 rue Jean Burguet, 33075 Bordeaux Cedex, France

F. Deschamps · P. Rao · T. de Baère
Department of Interventional Radiology,
Institut Gustave Roussy, 39 rue Camille Desmoulins,
94805 Villejuif Cedex, France

V. Brouste
Department of Biostatistics, Institut Bergonié,
229 cours de l'Argonne, 33076 Bordeaux Cedex, France

Introduction

Minimally invasive techniques have been developed for the treatment of unresectable primary and secondary lung tumors mostly for patients with advanced-stage disease or comorbidities that contraindicate surgery [1–3]. Radiofrequency ablation (RFA) is a local treatment available used for primary and metastatic malignancies [4–11]. RFA induces localized ionic agitation in the tissue through the oscillation of the applied alternating electrical current. It is this ionic agitation that leads to a progressive increase in temperature, resulting in cellular death. Recent results indicate that RFA in the lung is well-tolerated and provides a high rate of local tumor control [12–16]. Because the tumor and the surrounding ablated lung tissue remain in place, imaging follow-up is necessary to evaluate the local efficacy of the treatment. Due to the ablation of the margins to ensure total treatment of the tumor, normal tissue surrounding the tumor undergoes coagulation necrosis. This leads to a size increase of the imaged abnormality on the

first post-RFA follow-up compared with pretreatment imaging. Intratumoral hemorrhage also contributes to postinterventional increase in lesion size. At subsequent follow-up, the ablation zone decreases progressively in size. However, in some cases, no significant decrease is observed, and the ablation zone appears to be larger than before treatment. Even in the case of a total treatment without any residual viable tissue, a measurement based on RECIST (Response Evaluation Criteria in Solid Tumors) [17] criteria is not always a reliable measure of ablation success. As a result, it is essential to identify the computed tomography (CT) patterns of lung tumors after RFA to distinguish total ablation from local tumor progression. This study describes the different CT patterns of lung tumors treated with RFA.

Materials and Methods

Patients

Between October 2002 and October 2007, 198 consecutive patients (124 male and 74 female, mean age 63.4 ± 13 years) with 350 lung tumors underwent RFA, and clinical and imaging data were recorded prospectively. Overall, 82.8% of the tumors were metastatic from various origins (rectum and colon 43.9%; kidney 17.1%; and sarcoma 12.8%), and 17.2% were primary non–small cell carcinomas.

Preablation Assessment

The decision to perform RFA was taken after a multidisciplinary discussion with members of the thoracic surgery, medical oncology, radiation oncology, and radiology departments. All patients treated were discussed jointly before a decision was taken, and then the radiologist informed the patient of the risks, complications, and benefits of the procedure. An anesthetic consultation and thoracic CT were programmed for the month preceding the scheduled intervention. We obtained approval from the local Institutional Review Board to perform CT-guided RFA and to report the relevant data regarding these procedures. Informed consent was obtained from all patients.

RFA Procedure

All tumors were treated with RFA under CT guidance (HiSpeed; GE Medical Systems Milwaukee, WI). All RFA procedures were performed with the patient under general anesthesia. Prone, supine, or lateral positions were used to obtain the shortest access route to the tumor. Four grounding pads were placed on the patient's thighs. The RFA electrodes (LeVeen; Boston Scientific, Natick, MA) used were 14-gauge multitine expandable electrodes that were 15 cm long with a 2.0, 3.0, 3.5, or 4.0 cm array diameter when fully expanded. In addition, a LeVeen CoAccess electrode (Boston Scientific) with a 15 cm–long, 14-gauge insulated diamond tip–guiding needle was available with 3, 3.5, and 4.0 cm diameter RFA electrodes that could be inserted after retrieval of the stylet. Electrode size was always chosen to be at least 15 mm larger than the largest tumor diameter when possible. When several tumors had to be treated for the same patient in the same session, the size of the electrode was chosen according to the size of the largest tumor. The same electrode was used for the other tumors, with deployment tailored to 15 mm larger than the tumor. Real-time CT guidance without CT fluoroscopy was used to place the electrode, to image array deployment, and to monitor treatment.

RFA treatment was performed by applying a treatment algorithm dedicated to the lung that has been reported elsewhere [16]. In brief, this algorithm uses incremental power delivery and takes into account the size of the electrode and the location of the tumor in relation to the pleura. We delivered treatment until a major increase in impedance occurred. If this impedance increase occurred in <15 min, a second RFA delivery was performed in the same location, with 70% of the maximum power delivered to obtain this increase, until a new major increase in impedance occurred. If necessary, multiple overlapping ablations were performed in different portions of the tumor in numeric order (range 1–4). Local complications during the treatment, such as alveolar hemorrhages in the treatment area, were noted.

Prophylactic antibiotics, including clavulanate (2 g/d; Augmentin; Glaxo Smith Kline) and ofloxacin (400 mg/d; Oflocet, Sanofi-Avantis), were routinely administered intravenously during the procedure and then orally 3 days afterward.

CT Imaging Method

All patients were examined with CT imaging 2 days after treatment and then at 2, 4, 6, 9, and 12 months. From 2002 to 2005, CT examinations were performed with a spiral CT scanner (HiSpeed). Scanning was performed at 120 kV and 270 mA. Contiguously reconstructed sections (1:1 pitch) were obtained through the thorax in a single breath hold with 5-mm collimation and with or without injection of a contrast medium. For contrast-enhanced studies, patients received 100 ml of the contrast material (Iopamiron 370 [Bracco] or Ultravist 370 [Bayer Schering Pharma]) at a flow rate of 2–3 ml/s. From 2005 onward, CT scans were performed with a 16-slice multidetector row helical CT scanner (LightSpeed; GE Medical Systems) with 1.25-mm collimation at 120 kV and 350 mA. All follow-up CT scans

were performed on the same CT unit. After the first year, CT imaging was performed every 6 months.

Image Analysis

CT scans were evaluated separately by two radiologists (a junior in the fourth year of fellowship and a senior with 10 years of experience). CT images were read prospectively by the senior radiologist and retrospectively by the junior radiologist for each interval of 2, 4, 6, and 12 months. Subsequent CT scans performed after 12 months were not included in this analysis. In cases of interobserver disagreement, final decisions were reached by way of consensus. The pattern and the size of the treated area were evaluated at each imaging follow-up. Tumors with a largest diameter $\leq$2 cm were analyzed separately from tumors >2 cm. The CT shape of the treated area was classified as atelectasis, cavitation, disappearance, fibrosis, or nodule as described below:

1. Atelectasis (Fig. 1A–F): Ventilatory disturbance in a segment with increased attenuation surrounding the ablated tumor, thus preventing analysis of the RFA-ablated tumor.
2. Cavitation (Fig. 2A–C): An air-filled cavity with thick or thin walls appearing in the location of the ablated area. Cavitation may be incomplete and only in one part of the ablated volume.
3. Disappearance: The RFA zone is impossible to depict. No sequel of the ablation zone is seen
4. Fibrosis (Fig. 3A–E): The RFA zone looses its sphericity and becomes elongated and linear with or without peripheral spicules.
5. Nodule (Fig. 4A–D): After treatment, the RFA zone remains spherical with no signs of retraction. The frequency of each classification was recorded for the RFA zone, and we used χ^2 test to compare the different types of images across size of treated tumors ($\leq$ or >2 cm) and at various follow-up points.

The two-dimensional volume size (longest diameter and its perpendicular) of the ablation measured by way of CT at day 2 was used as the baseline value for follow-up. An incomplete treatment was defined as any increase in the size of any one or both of the two-dimensional measurements found on follow-up CT examinations or as an appearance of any irregular, nodular, or eccentric focus at the margin of the ablation zone. Stability or any decrease in size was considered as complete treatment.

No histologic control was performed after RFA, except in the case of two RFA-ablated tumors. For these two patients, lung surgery was decided due to the presence of new tumors that were not treatable with RFA. Resection of the RFA volume was performed at the same time as the planned metastasectomy.

If patients started chemotherapy or hormonotherapy for their tumors after RFA, they were excluded from the imaging analyses to avoid any influence of such treatment on the imaging patterns of the RFA zone.

Statistical Methods

Follow-Up

Median Follow-up Time was Calculated with the Inversed Kaplan–Meier technique [18].

Survival

Survival was calculated with the Kaplan–Meier technique and SPSS 18.0 software as the time between RFA and the date of death or last news regarding the patient. Patients who started chemotherapy or hormonotherapy after RFA were not excluded from this analysis.

Results

One hundred ninety-eight patients with 350 lung tumors were treated overall. At 1-year follow-up, 127 patients with 210 lesions remained in the analysis: 24 patients had died (19 from progression); 21 had started a systemic treatment (chemotherapy, hormonotherapy) within the study period; and 26 other patients had missing follow-up values. Median follow-up time was 36 months (range 32 to 40). The

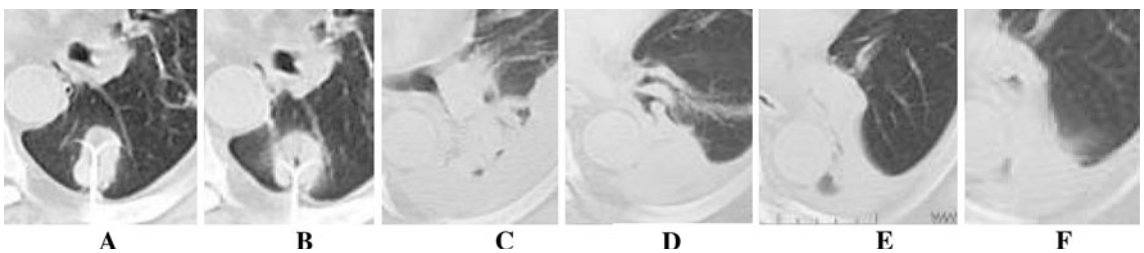

Fig. 1 Atelectasis: treatment (**A**, **B**), follow-up 48 h (**C**), 4 months (**D**), 6 months (**E**), 9 months (**F**)

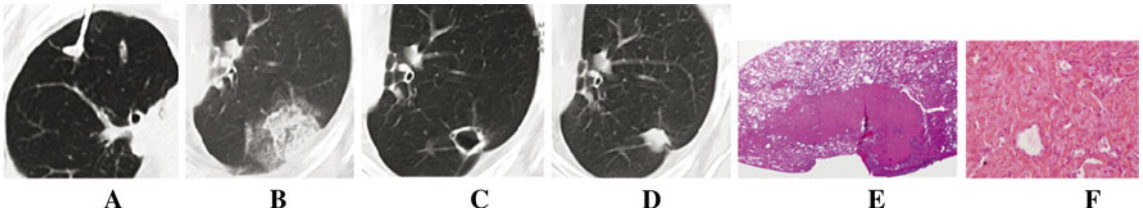

Fig. 2 Cavitation: treatment (**A**), follow-up 48 h (**B**), 4 months (**C**), 6 months (**D**): nodular pattern, histological analysis of the nodule (**E** H&E ×20, **F** H&E ×200): fibroblasts and collagen, no tumoral cells

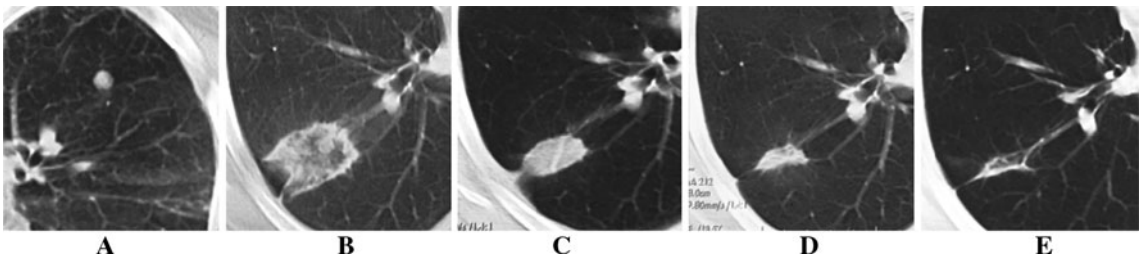

Fig. 3 Fibrosis: before treatment (**A**), follow-up 48 h (**B**), 4 months: nodular pattern (**C**), 6 months (**D**) and 12 months (**E**): fibrous pattern

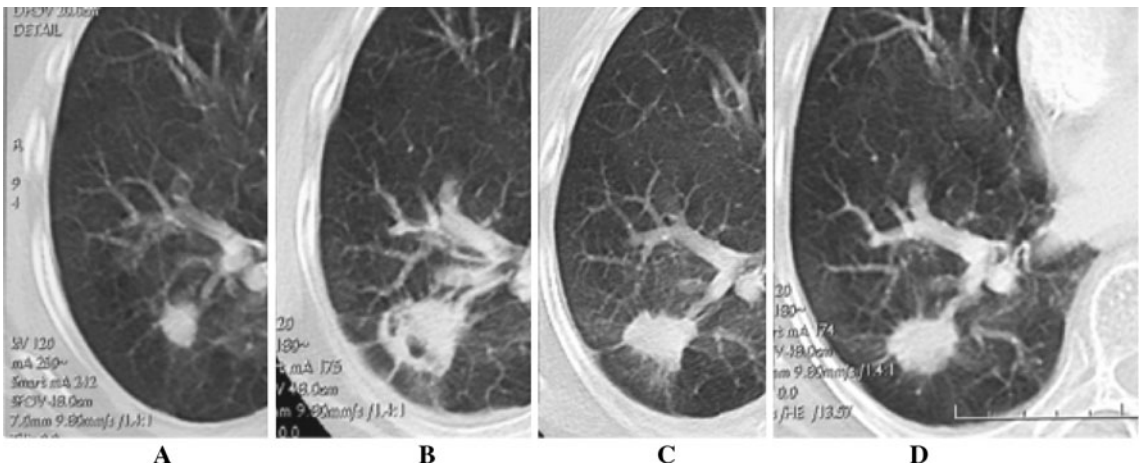

Fig. 4 Nodule: before treatment (**A**), follow-up 4 months (**B**), 6 months (**C**), 12 months (**D**)

probability of survival at 2, 3, and 5 years was 72%, 60%, and 51%, respectively.

Before treatment, all tumors were characterized as nodular. Overall, 73.1% of the tumors were ≤2 cm, and 26.9% of tumors were >2 cm. Mean tumor size was 15 mm ± 9 mm.

The location of the tumor related to the pleura was as follows: intraparenchymatous (71.7%), pleural contact inferior to 50% (21.7%), and pleural contact superior to 50% (6.6%). One hundred sixty-eight of the initial 198 patients were treated in one session (unilateral tumors $n = 152$; bilateral tumors $n = 16$), and 30 were treated in two different sessions (all were bilateral tumors). When both lungs were treated during the same procedure, the second lung was punctured if no complication occurred after treatment of the first lung. Tumors >2 cm were treated with one ablation in 15%, with two overlapping ablations in 45%, with three overlapping ablations in 34%, and with four overlapping ablations in 6% of patients. The number of patients followed-up for evaluation of imaging patterns decreased progressively with time due to death, missing values, or the start of chemotherapy (Table 1). Morphologic patterns of the treated tumors ≤2 cm and >2 cm, which are

Table 1 Number of patients followed-up and RFA zone

No. of months	No. of patients	RFA zone
2	189	287
4	181	279
6	169	259
9	149	233
12	127	210

Table 2 Different features after RFA of tumors ≤2 cm

RFA zones	Time of follow-up (mo)				
	2 (n = 211)	4 (n = 201)	6 (n = 190)	9 (n = 175)	12 (n = 162)
No. of fibroses (%)	24 (11.4)	56 (27.9)	85 (44.7)	88 (50.3)	95 (58.6)
No. of nodules (%)	144 (68.2)	125 (62.2)	93 (48.9)	76 (43.4)	59 (36.4)
No. of cavitations (%)	25 (11.8)	12 (6)	5 (2.6)	5 (2.9)	4 (2.5)
No. of GGOs (%)	13 (6.2)				
No. of atelectases (%)	5 (2.4)	6 (3)	4 (2.1)	3 (1.7)	2 (1.2)
No. of disappearances (%)	0	2 (1)	3 (1.6)	3 (1.7)	2 (1.2)

Table 3 Different features after RFA of tumors >2 cm

RFA zones	Time of follow-up				
	2 (n = 76)	4 (n = 78)	6 (n = 69)	9 (n = 58)	12 (n = 48)
No. of fibroses (%)	5 (6.6)	5 (6.4)	7 (10.1)	9 (15.5)	11 (22.9)
No. of nodules (%)	53 (69.7)	60 (76.9)	55 (79.7)	45 (77.6)	35 (72.9)
No. of cavitations (%)	11 (16)	9 (11.5)	4 (5.8)	1 (1.7)	1 (2.1)
No. of GGOs (%)	3 (3.9)				
No. of atelectases (%)	4 (5.3)	4 (5.1)	3 (4.3)	3 (5.2)	1 (2.1)
No. of disappearances (%)	0	0	0	0	0

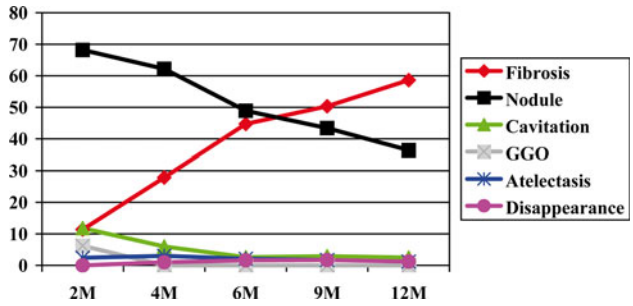

Fig. 5 Patterns of RF ablation zone for tumors ≤2 cm according to duration of follow-up

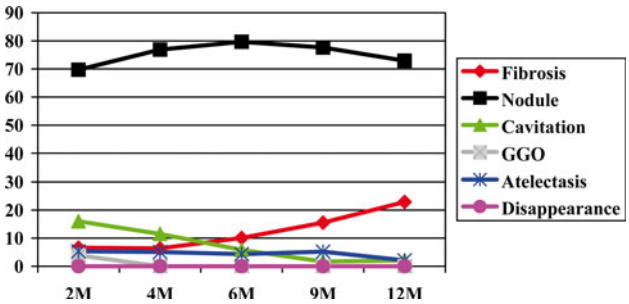

Fig. 6 Patterns of RF ablation zone for tumors >2 cm according to duration of follow-up

listed in Tables 2 and 3 and Figs. 5 and 6, display the features obtained at 2, 4, 6, 9, and 12 months. CT imaging 2 days after treatment shows a tumor completely surrounded by peripheral ground-glass opacity (GGO) in all patients.

CT imaging 2 months after treatment shows a nodular appearance of the RFA zone in 68.6% of the RFA zones (n = 197) regardless of the initial size of the treated tumor, whereas GGOs persisted in 5.5% of the lesions. In addition, 12.5% of the RFA zones evolved to cavitation (n = 3) and 3.1% to atelectasis (n = 9), and it is noticeable that all of these were located in the inferior lobe.

CT Imaging Results 4 to 6 Months After Treatment

Fibrotic scars were significantly more frequent (44.7%, p = 0.0000003 for tumors ≤2 cm than for larger tumors), with some rare cases (0.7–1.2%) of disappearance of the post-RFA zone. For tumors >2 cm, the aspect of the RFA zone was significantly more nodular than for smaller tumors (79.7%, p = 0.000009). Some of the cavitated RFA zones at 2 months became nodules or fibrosis at 4 and 6 months, with resolution of the previous cavity (Figs. 2D, 7). Of the 36 cavitations at 2 months, 6 had become a fibrosis at 4 months and 16 had become a nodule. At 6 months, 5 additional cavitations had become a nodule, and 1 had become a fibrosis. Only 8 cavitations remained at 6 months.

CT Imaging Results 6 to 12 Months After Treatment

Almost one quarter (22.9%) of the tumors >2 cm became fibrous, but a significant majority (p = 0.000008) remained

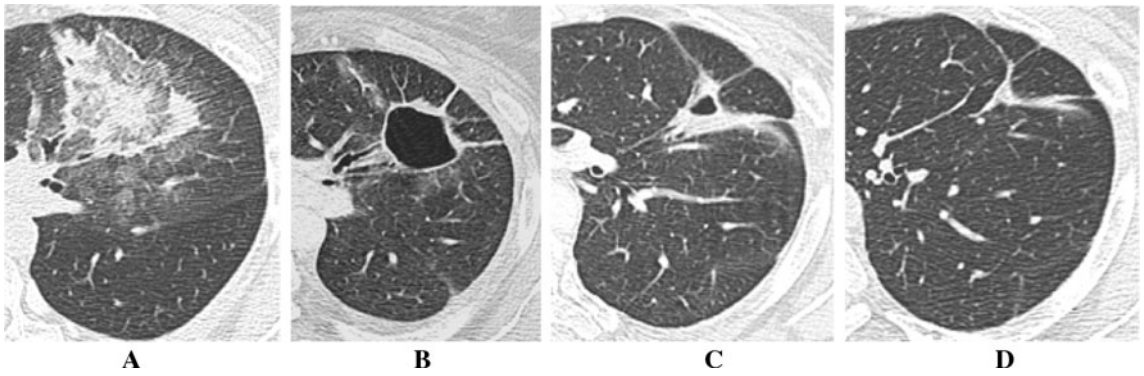

Fig. 7 From cavitation to fibrous pattern: follow-up 48 h after RFA (**A**), 4 months (**B**), 9 months (**C**), 12 months (**D**)

nodular (72.9%). The trend was different for tumors ≤2 cm, where more than half became fibrous (58.6%, $p = 0.00001$), and 36.4% remained nodular. A small proportion (1.2%) of the RFA zones disappeared when the initial tumor had been ≤2 cm before treatment. Some of the cavitated RFA zones returned to a fibrous aspect. In one case, histologic examination after complete resection of a nodule filling a cavity showed only fibrous tissue (Fig. 2E, F). Among the cavities, 61% had become nodular (22 of 36) and 22% fibrous (8 of 36). At 1 year, only five images showed remaining cavitation.

Local Tumor Progression

In 28 tumors, incomplete ablation was documented by follow-up scans with clear evidence of increased size of the RFA zone on two subsequent follow-ups. Incomplete ablation was represented by the appearance of a nodular focus in fibrous pattern and cavitation (Fig. 8) at the margin of the ablation zone. At 1 year, 12 recurrences were noted. All patterns were concerned by incomplete ablation, including: 2 fibrosis, 2 cavitation, 7 nodules, and 1 atelectasis. Sixteen recurrences were noted after 1 year. Incomplete local treatment was discovered at a median of 10.6 months after treatment (range 2 to 41).

Complications

Three quarters of all procedures involved immediate complications. Pneumothorax was the most frequent (52.9%), and 48.8% of these were drained. Twenty-three patients (representing 33 tumors) presented an alveolar hemorrhage related to a puncture in the treatment area.

Discussion

Treatment and Follow-Up

The thermal properties of the lung are a consequence of the presence of air-filled spaces. The presence of air means a lower thermal inertia and a greater electrical impedance than in other tissues**.** In this context, the surrounding air in the lung insulates the heated volume thermally and electrically, and it has been demonstrated that tissue characteristics affect ablation outcomes, with a larger volume of ablation in the lung than in the kidney or soft tissues for a given quantity of energy [19]. In rabbit lung [20], an inflammatory reaction occurs after RFA. During the first weeks after treatment, the reaction appears as a progressive organization of the coagulated zone with granulation tissue and local dilatation of blood vessels. This leads to an

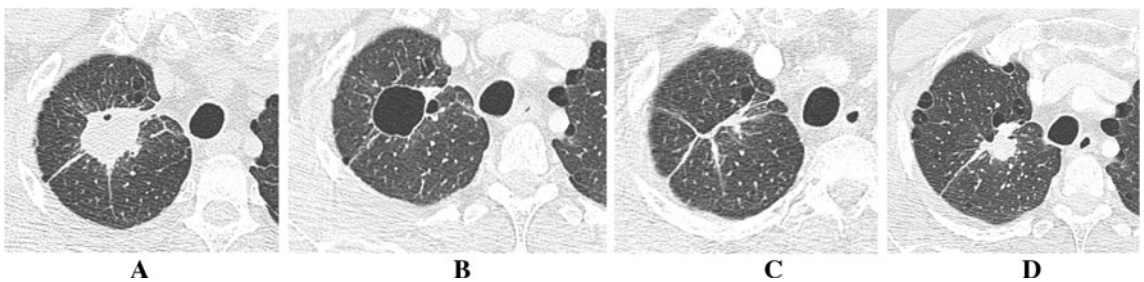

Fig. 8 Local tumor progression: follow-up 2 month after RFA: nodular pattern (**A**), 4 months: cavitation (**B**), 9 months: fibrous pattern (**C**), 12 months: local tumor evolution (**D**)

increase in size of the ablated zone with perinodular GGOs. After 1 month, fibrous tissue progressively replaces the coagulation necrosis. Animal experiments have generally shown excellent prediction of tissue response to thermal injury using a CT scanner [21].

Various publications [2, 22, 23] have confirmed the clinical utility of a CT scan in the follow-up of lung tumors treated by RFA. After an initial increase in size due to inflammation during the first 2 months, the ablated zone usually recedes progressively. However, the decrease in size is moderate and does not always occur, with the size of the RFA zone remaining unchanged with time. The same absence of involution has been demonstrated in liver and kidney tumors, even with long-lasting RFA zones that are still present after several years [4, 9, 10]. Compared with other organs, such as the liver and the kidney, various features of RFA zones are specific to the lung. We classified them into five main patterns of evolution after 2 months. The fibrous and nodular patterns are the most frequent, although the main factor predictive of evolution is the initial size of the tumor. Location of the tumor (intraparenchymatous, pleural contact <50% or >50%) did not significantly influence the final aspect.

GGOs

RFA-induced GGOs include the normal parenchyma surrounding the tumor. GGOs were seen on the first control at 48 h in all cases, as has been shown in previous reports [24]. These opacities correspond to congestion, edema, hemorrhagic rim, inflammatory cell infiltration, and necrotic lesions induced by thermal ablation, as described in animal-based studies showing a correlation between CT and pathologic findings [21]. The demarcation with the nonablated tissues is clear. The tumors were centered on the RFA-ablated areas, after which we expect complete ablation. The size of the ground-glass appearance on initial CT is useful to predict treatment success [25] because it is twice as long and twice as wide as the tumor [16], Anderson et al. [26] described that a circumferential GGO margin of >5 mm is the minimal margin required to ensure complete tumor ablation. A parenchymatous opacity occurs rapidly beginning the week after RFA with a similar size as the GGOs [24], and at 2 months the GGOs have generally disappeared (94.5% of the patients in our series).

Evolution After 2 Months

We used "fibrosis" as a radiologic definition without any histological proof. It corresponds to a change in the primary shape of the RFA zone and indicates a progressive shrinkage of the treated volume with reabsorption of the coagulated area, including the tumor. This pattern may appear 2 months after treatment but is more frequent after 4 months. With regard to tumor size before treatment, tumors ≤2 cm became fibrous more rapidly and more frequently than larger ones, probably because the volume of coagulated tissues to reabsorb is lower. Recently it was also demonstrated on *ex vivo* lung tissues that RFA induces an approximate volume decrease of 27–75% [27]. In this study, contraction in normal lung was more significant than in liver. The explanation given by the investigators was that contraction in the lung may be more related to architectural distortion and collapse, whereas in the liver it is primarily caused by dehydration.

In contrast, the nodular pattern is more frequent with larger tumors (>2 cm). The nodular pattern is more ambiguous, and it might be difficult to differentiate this posttreatment aspect from possible incomplete treatment owing to the fact that all local recurrences except one were nodular in shape. To resolve this issue, an intravenous contrast agent may be used to differentiate nonenhancing scars from enhancing residual tumor [22]. In this regard, nodular perfusion studies with dedicated software can probably help [28] but are not used in routine practice. Contrast-enhanced magnetic resonance imaging (MRI) has demonstrated an ability to differentiate between benign and malignant lung tumors [29] and can be used in follow-up as reported by Van Sonnenberg [30], who described decreased or no enhancement on MRI scans after RFA compared with preprocedural scans. A recent study suggests that diffusion-weighted MRI may predict the response to RFA for lung tumors [31]. However, these results must be confirmed in larger series. Comparing anatomic and metabolic changes with ^{18}F-FDG PET/CT is another option, but the extensive initial inflammatory reaction interferes in the assessment of treatment response and makes it more difficult than in other settings. With animals, the best timing to avoid inflammatory changes was found to be early after RFA (12–24 h) or later than 6 to 8 weeks [32]. Clinical validation in humans has not yet been established conclusively [33, 34].

The challenge to identify areas of incomplete ablation remains in this nodular pattern owing to the evident limitations of different imaging techniques to identify microscopic disease. Accuracy is limited by spatial resolution, partial-volume effect, and contrast resolution. In a small series, neither CT, nor MRI, nor ^{18}F-FDG PET/CT was able to identify residual microscopic disease 1 or 2 weeks after treatment [35].

Cavitation has been reported to occur more frequently when the tumor is close to a segmental bronchus [24]. Other reported factors contributing to cavitation are peripheral tumors, primary cancer, and pulmonary emphysema [36]. In our series, we found no influence of the location of the tumor, and a fistula with a bronchus was identified on CT scan in only six patients. These six patients presented

coughing and unclean expectorations, without fever or clinical signs of pneumonia or abscesses, for 1 to 2 months after the treatment, indicating possible drainage of the ablated tumor into a bronchus. In the 30 other cavitations observed at 2 months, the patients were completely asymptomatic. There was no influence of the size of the tumor before treatment to explain the appearance of a cavity.

For tumors >2 cm, we suspected that multiple overlapping RFA applications may have resulted in overtreatment of the region with an increased risk of bronchial fistula, but the influence of multiple RFA applications was not statistically significant, even if it is noteworthy that all of the cavitation patients received ablation in more than one location compared with 81% of the other categories (nodules, fibrosis, atelectasis).

Steinke et al. [23] reported that the rate of cavitation was higher if there was an increase >200% of the treatment zone size 1 week after RFA. In addition, whereas a cavity persisting in the lung may be considered as a risk of superinfection, cavitation is not definitive in most patients. In our series, 64.7% of the cavitations had become a nodule or fibrosis at 4 months, whereas at 12 months only 2.4% of the cavitations remained; no superinfection of the cavitation was encountered.

Concerning atelectasis, an area of obstructive pneumonitis had developed in place of the tumor, thereby complicating interpretation. In our experience, atelectasis occurs only on a lobar inferior tumor, and pleuresis was not systematically associated. Fibroscopy could be useful to verify the absence of endobronchial invasion after an incompletely treated tumor.

Local tumor progression was defined as an increase in tumor size after a posttherapeutic period of stability of approximately 6 months in general. Unfortunately, our analysis shows that there is not one post-RFA ablation imaging pattern that guarantees that treatment is complete.

All the different patterns can be associated with local tumor progression, but more frequently in the case of a nodular one. Fibrous evolutions and cavitations, in which the primary tumor is thought to have completely resolved, demonstrated some surprising regrowth in zones where the initial shape of the tumor had entirely disappeared. In contrast, a regrowth of a nodular post-RFA zone can be easily understood as an incompletely treated viable tumor that has continued to grow. Consequently, there is no pattern that warrants a clinical decision to discontinue follow-up after lung RFA. A minimum of 1-year follow-up appears necessary because late recurrence has been reported.

Limitations of the Study

A possible limitation of our study is that no biopsies were performed. Some classifications could have been confirmed with histologic analyses, especially in the case of nodular evolution, although there are some drawbacks with biopsies if an inadequate amount of tissue is sampled.

Conclusion

RFA for lung tumors results in persistent radiologic abnormalities, which appear more difficult to interpret than for tumors of the liver or kidney due to wide variety of patterns encountered. All post-RFA features described may lead to residual or recurrent disease despite the appearance of complete ablation in some cases. The challenge for imaging remains the identification of these areas of incomplete ablation to inhibit local tumor progression arising from residual microscopic disease and the discovery of recurrences many months after treatment. Careful and extended follow-up imaging of tumors treated with RFA remains necessary.

Acknowledgements We thank Pippa McKelvie-Sebileau for help with the manuscript.

Conflict of interest The authors declare that they have no conflict of interest.

References

1. Abbas G, Schuchert MJ, Pennathur A et al (2007) Ablative treatments for lung tumors: radiofrequency ablation, stereotactic radiosurgery, and microwave ablation. Thorac Surg Clin 17:261–271
2. Dupuy DE, Mayo-Smith WW, Abbott GF et al (2002) Clinical applications of radio-frequency tumor ablation in the thorax. Radiographics 22(Spec No.):S259–S269
3. Rose SC, Thistlethwaite PA, Sewell PE et al (2006) Lung cancer and radiofrequency ablation. J Vasc Interv Radiol 17:927–951
4. de Baère T, Elias D, Dromain C et al (2000) Radiofrequency ablation of 100 hepatic metastases with a mean followup of more than 1 year. AJR Am J Roentgenol 175:1619–1625
5. Lencioni RA, Allgaier HP, Cioni D et al (2003) Small hepatocellular carcinoma in cirrhosis: randomized comparison of radiofrequency thermal ablation versus percutaneous ethanol injection. Radiology 228:235–240
6. McGrane S, McSweeney SE, Maher MM (2008) Which patients will benefit from percutaneous radiofrequency ablation of colorectal liver metastases? Critically appraised topic. Abdom Imaging 33:48–53
7. Suppiah A, White TJ, Roy-Choudhury SH et al (2007) Long-term results of percutaneous radiofrequency ablation of unresectable colorectal hepatic metastases: final outcomes. Dig Surg 24:358–360
8. Dupuy DE, Goldberg SN (2001) Image-guided radiofrequency tumor ablation: challenges and opportunities. Part II. J Vasc Interv Radiol 12:1135–1148
9. Zagoria RJ, Traver MA, Werle DM et al (2007) Oncologic efficacy of computed tomography (CT)-guided percutaneous radiofrequency ablation of renal cell carcinomas. AJR Am J Roentgenol 189:429–436

10. Park S, Cadeddu JA (2007) Outcomes of radiofrequency ablation for kidney cancer. Cancer Control 14:205–210
11. Link TM, de Mayo R, O'Donnell RJ (2007) Radiofrequency ablation: an alternative for definitive treatment of solitary bone metastases. Eur Radiol 17:3012–3013
12. Suh R, Reckamp K, Zeidler M et al (2005) Radiofrequency ablation in lung cancer: promising results in safety and efficacy. Oncology (Williston Park) 19(11 Suppl 4):12–21
13. Simon CJ, Dupuy DE, DiPetrillo TA et al (2007) Pulmonary radiofrequency ablation: long-term safety and efficacy in 153 patients. Radiology 243:268–275
14. Yan TD, King J, Sjarif A et al (2006) Percutaneous radiofrequency ablation of pulmonary metastases from colorectal carcinoma: prognostic determinants for survival. Ann Surg Oncol 13:1529–1537
15. Yan TD, King J, Sjarif A et al (2007) Treatment failure after percutaneous radiofrequency ablation for nonsurgical candidates with pulmonary metastases from colorectal carcinoma. Ann Surg Oncol 14:1718–1726
16. de Baère T, Palussière J, Auperin A et al (2006) Midterm local efficacy and survival after radiofrequency ablation of lung tumors with minimum follow-up of 1 year: prospective evaluation. Radiology 240:587–596
17. Therasse P (2002) Evaluation of response: new and standard criteria. Ann Oncol 13(Suppl 4):127–129
18. Shuster JJ (1991) Median follow-up in clinical trials. J Clin Oncol 9:191–192
19. Ahmed M, Liu Z, Afzal KS et al (2004) Radiofrequency ablation: effect of surrounding tissue composition on coagulation necrosis in a canine tumor model. Radiology 230:761–767
20. Goldberg SN, Gazelle GS, Compton CC et al (1995) Radiofrequency tissue ablation in the rabbit lung: efficacy and complications. Acad Radiol 2:776–784
21. Yamamoto A, Nakamura K, Matsuoka T et al (2005) Radiofrequency ablation in a porcine lung model: correlation between computed tomography (CT) and histopathologic findings. AJR Am J Roentgenol 185:1299–1306
22. Suh RD, Wallace AB, Sheehan RE et al (2003) Unresectable pulmonary malignancies: computed tomography (CT)-guided percutaneous radiofrequency ablation: preliminary results. Radiology 229:821–829
23. Steinke K, Glenn D, King J et al (2004) Percutaneous imaging-guided radiofrequency ablation in patients with colorectal pulmonary metastases: 1-year follow-up. Ann Surg Oncol 11:207–212
24. Bojarski JD, Dupuy DE, Mayo-Smith WW (2005) computed tomography (CT) imaging findings of pulmonary neoplasms after treatment with radiofrequency ablation: Results in 32 tumors. AJR Am J Roentgenol 185:466–471
25. Lee JM, Jin GY, Goldberg SN et al (2004) Percutaneous radiofrequency ablation for inoperable non-small cell lung cancer and metastases: preliminary report. Radiology 230:125–134
26. Anderson EM, Lees WR, Gillams AR (2009) Early indicators of treatment success after percutaneous radiofrequency of pulmonary tumors. Cardiovasc Intervent Radiol 32:478–483
27. Brace CL, Diaz TA, Hinshaw JL et al (2010) Tissue contraction caused by radiofrequency and microwave ablation: a laboratory study in liver and lung. J Vasc Interv Radiol 21:1280–1286
28. Hakimé A, Peddi H, Hines-Peralta AU et al (2007) computed tomography (CT) perfusion for determination of pharmacologically mediated blood flow changes in an animal tumor model. Radiology 243:712–719
29. Schaefer JF, Vollmar J, Schick F et al (2004) Solitary pulmonary nodules: Dynamic contrast-enhanced MR imaging–perfusion differences in malignant and benign lesions. Radiology 232:544–553
30. VanSonnenberg E, Shankar S, Morrison PR et al (2005) Radiofrequency ablation of thoracic lesions. Part 2. Initial clinical experience: technical and multidisciplinary considerations in 30 patients. AJR Am J Roentgenol 184:381–390
31. Okuma T, Matsuoka T, Yamamoto A et al (2009) Assessment of early treatment response after computed tomography (CT)-guided radiofrequency ablation of unresectable lung tumours by diffusion-weighted MRI: a pilot study. Br J Radiol 82:989–994
32. Okuma T, Matsuoka T, Okamura T et al (2006) ^{18}F-FDG small-animal PET for monitoring the therapeutic effect of computed tomography (CT)-guided radiofrequency ablation on implanted VX2 lung tumors in rabbits. J Nucl Med 47:1351–1358
33. Okuma T, Okamura T, Matsuoka T et al (2006) Fluorine-18-fluorodeoxyglucose positron emission tomography for assessment of patients with unresectable recurrent or metastatic lung cancers after computed tomography (CT)-guided radiofrequency ablation: preliminary results. Ann Nucl Med 20:115–121
34. Avril N (2006) ^{18}F-FDG PET after radiofrequency ablation: Is timing everything? J Nucl Med 47:1235–1237
35. Hataji O, Yamakado K, Nakatsuka A et al (2005) Radiological and pathological correlation of lung malignant tumors treated with percutaneous radiofrequency ablation. Intern Med 44:865–869
36. Okuma T, Matsuoka T, Yamamoto A et al (2007) Factors contributing to cavitation after computed tomography (CT)-guided percutaneous radiofrequency ablation for lung tumors. J Vasc Interv Radiol 18:399–404